Nonlinear effects in dynamics of micromechanical gyroscope

Roman Starosta, Grażyna Sypniewska-Kamińska, Jan Awrejcewicz

Abstract: Resonant sensors basing on microstructures and belonging to microelectromechanical systems (MEMS) have been developed in recent years. The paper deals with dynamics of micro-gyroscope being a sensor designed for measuring the angular displacement. Such device is used for the attitude control of a moving object. Vibration of the basic measuring element suspended on a set of two pivoted and mutually orthogonal axes is the object of our study. One coordinate of the angular velocity of the support can be measured by the MEMS system. Since a resonance phenomenon is the desirable state of work of this sensor, the elastic properties of the support should be appropriately designed. Therefore, it is important to consider also the nonlinear behaviour of the system. It is assumed that the elastic features of the sensor suspension are weakly nonlinear. The equations of motion of the micromechanical sensor have been derived using the Lagrange formalism. The approximated solutions obtained using multiple scales method allow to investigate the resonant behaviour of the system.

1. Introduction

Gyroscopes are present in a broad range of engineering systems such as air vehicles, automobiles, and satellites to track their orientation and control their path. Besides the directional gyroscopes there are variety kinds of gyroscopes (e.g. mechanical, optical and vibrating) that are being used to measuring the angular velocity. The critical part of the conventional mechanical gyroscope is a wheel spinning at a high speed. Therefore, conventional gyroscopes although accurate are bulky and very expensive and they are applicable mainly in the navigation systems of large vehicles, such as ships, airplanes, spacecrafts, etc.

Progress in micromachining technology embraces the development of the miniaturized gyroscopes with improved performance and low power consumption that allow the integration with electronic circuits. Their manufacturing cost are also significantly lower [1–2]. Such type of gyroscopes belongs to broad class of microelectromechanical systems (MEMS). Practically, any device fabricated using photo-lithography based techniques with micrometer scale features that utilizes both electrical and mechanical functions could be considered as MEMS.

The operating principle of vibrating gyroscopes is based on the transfer of the mechanical energy among two vibrations modes via the Coriolis effect which occurs in the presence of

a combination of rotational motions about two orthogonal axes. The drive mode is mainly generated employing the electrostatic actuation mechanism.

In the present work, we conduct an analysis of dynamics of a MEMS gyroscope. This micro device is a torsional resonator. Resonance is the desirable state of work of this sensor, so the elastic properties should be appropriately matched. Designing the resonator, only linear elasticity is taken into account. There arises the question what is the significance of the nonlinear properties of resilient resonator elements. Therefore, we propose the mathematical model describing motion of the MEMS gyroscope taking into account the nonlinear effects generated by the elastic properties of the suspension elements. The main objective of the paper is to obtain and to examine the resonant responses of the considered system.

2. Description of micromechanical gyroscope

MEMS gyroscope, whose scheme is presented in Fig. 1, with the sensing plate suspended on a set of two pivoted and mutually orthogonal axes is studied. The active gimbal is supported by two torsional connectors that are anchored to the substrate and designate the drive axis, so that the gimbal oscillates only about this axis. The sensing plate is linked to the gimbal via two torsional joints determining the sense axis and allowing to oscillate about this axis independent from the gimbal position. Both the sensing plate and the gimbal are treated further as rigid bodies.

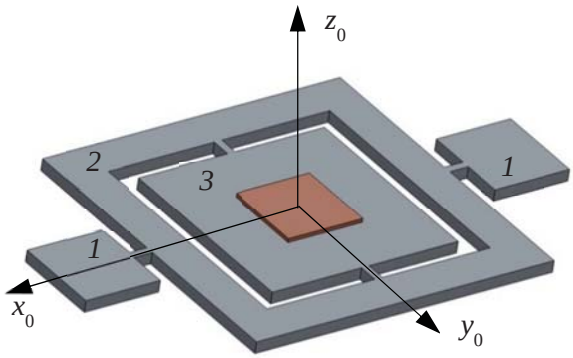

Figure 1. Micromechanical gyroscope suspended on a set of two pivoted and mutually orthogonal pivot axes; 1 – anchor, 2 – gimbal, 3 – sensing plate.

The kinematics of the gyroscope is best to understand by introducing three reference frames shown in Fig. 2. They have the common origin at the point O. In the frame F_0 with the coordinate system $Ox_0y_0z_0$ the anchors are motionless. The frame F_1 with the coordinate system $Ox_1y_1z_1$ is fixed to the intermediate pivoted support, whereas the frame F in which it is assumed the coordinate system $Oxyz$ is rigid connected with the sensing plate. The frame F_1 which can oscillate about the drive axis

x_0 is presented in position rotated by Φ counterclockwise, and the frame F oscillating around the sense axis y_1 is shown in position being a result of the rotation by Θ, also counterclockwise.

The substrate, in general, can rotate about a fixed pivot axis. Let as assume that its angular velocity $\mathbf{\Omega}_z$ projected on the axes of the frame F_0 is $\mathbf{\Omega}_z = [0,0,\Omega_z]^T$ where Ω_z is to be measured.

The absolute gimbal angular velocity $\mathbf{\Omega}_1$ is a superposition of the substrate rotation and own rotation about the drive axis. Projecting it onto the axes of the frame F_1, we obtain

$$\mathbf{\Omega}_1 = \left[\Phi, \Omega_z \sin\Phi, \Omega_z \cos\Phi\right]^T. \tag{1}$$

The absolute angular velocity $\mathbf{\Omega}$ of the sensing plate written in the reference frame F and being a result of the substrate motion, gimbal rotation and own rotation about y-axis is

$$\mathbf{\Omega} = \left[-\Omega_z \cos\Phi \sin\Theta + \cos\Theta\Phi, \Omega_z \sin\Phi + \Theta, \Omega_z \cos\Phi \cos\Theta + \Phi \sin\Theta\right]^T. \tag{2}$$

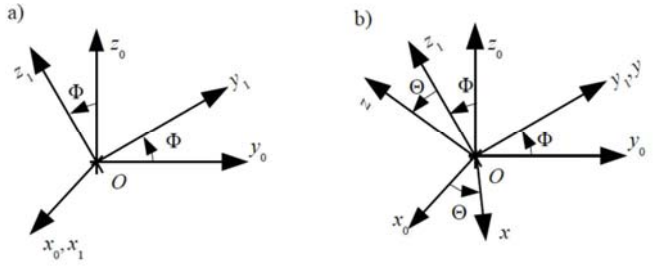

Figure 2. The angles of rotation Φ and Θ: (a) the rotation of F_1 by Φ about x_0-axis; (b) The rotation of F_2 by Θ around y_1.

3. Equations of motion

The considered microsystem has two degrees of freedom in motion with respect to the substrate. The rotation angles Φ(t) and Θ(t) are assumed to be the general coordinates. The point O that is the mass center both of the sensing plate and the gimbal is constantly at rest. The axes of reference frames F_1 and F are the principal axes of inertia of the gimbal and the plate, respectively. Therefore, the inertia tensors of each of the gyroscope part related to these axes are of diagonal form independent of the current system configuration. Let I_x, I_y and I_z denote moments of inertia of the gimbal about its principal inertia axes x_1, y_1 and z_1, whereas J_x, J_y and J_z stands for the principal moments of inertia of the senor plate i.e. with respect to the axes x, y and z. In other words, the inertia tensors of both gyroscope parts we can write as $\hat{\mathbf{I}} = diag(I_x, I_y, I_z)$ and $\hat{\mathbf{J}} = diag(J_x, J_y, J_z)$.

The kinetic energy of the system is a sum of two quadratic forms

$$T = \frac{1}{2}\left(\boldsymbol{\Omega}_1^T . \hat{\mathbf{I}} . \boldsymbol{\Omega}_1 + \boldsymbol{\Omega}^{\mathrm{T}} . \hat{\mathbf{J}} . \boldsymbol{\Omega}\right). \tag{3}$$

Substituting formulas (1) and (2) into equation (3), we get

$$T = \frac{1}{2}\left(I_z\Omega_z^2(\cos\Phi)^2 + I_y\Omega_z^2(\sin\Phi)^2 + I_x\Theta^2\right) + \tag{4}$$
$$\frac{1}{2}\left(J_x\left(\Omega_z\cos\Phi\sin\Theta - \Phi\cos\Theta\right)^2 + J_z\left(\Omega_z\cos\Phi\cos\Theta + \Phi\sin\Theta\right)^2 + J_y\left(\Omega_z\sin\Phi + \Theta\right)^2\right).$$

Taking into account that the system mass center *O* is immovable and assuming that the elastic properties of all torsional connectors are nonlinear of cubic type, we can write the potential energy as follows

$$V = \frac{1}{2}k_{11}\Phi^2 - \frac{1}{4}k_{12}\Phi^4 + \frac{1}{2}k_{21}\Theta^2 - \frac{1}{4}k_{22}\Theta^4, \tag{5}$$

where k_{11}, k_{12} and k_{21}, k_{22} are elastic coefficients of the outer and the inner torsional connectors respectively.

The viscous effects of gas, which is confined between the rotating surfaces and the immovable ones, play the primary role in damping mechanism. The system is excited by the driving electrostatic torque $M_0 \sin(P\,t)$ applied to the drive gimbal.

The governing equations have been derived using Lagrange's equations of the second kind. Due to expected small values of angles Φ and Θ, we assume linear approximation of the trigonometric functions, whose arguments are these angles, making the equations of motion simpler of the following form

$$(I_x + J_x)\Phi + k_{11}\Phi - k_{12}\Phi^3 + C_1\Phi + (I_z - I_y + J_z - J_y)\Omega_z^2\Phi - (J_x + J_y - J_z)\Omega_z\Theta + \tag{6}$$
$$2(J_z - J_x)\Theta\Theta\Phi = M_0\sin(P\,t),$$

$$J_y\Theta + k_{21}\Theta - k_{22}\Theta^3 + C_2\Theta + (J_z - J_x)\Omega_z^2\Theta + (J_x + J_y - J_z)\Omega_z\Phi + (J_z - J_x)\Omega_z\Theta^2\Phi + \tag{7}$$
$$(J_x - J_z)\Theta\Phi^2 = 0,$$

where C_1 and C_2 are the damping coefficients.

It is convenient to transform the governing equations into the nondimensional form. For this purpose we introduce the dimensionless time $\tau = t\,\omega_1$ and the following dimensionless parameters:

$$p = \frac{P}{\omega_1},\ \omega_z = \frac{\Omega_z}{\omega_1},\ f_0 = \frac{M_0}{(I_x + J_x)\omega_1^2},\ c_1 = \frac{C_1}{(I_x + J_x)\omega_1},\ c_2 = \frac{C_2}{J_y\omega_1},\ \alpha_1 = \frac{k_{12}}{(I_x + J_x)\omega_1^2},$$

$$\alpha_2 = \frac{k_{22}}{J_y \omega_1^2},\ j_1 = \frac{I_z + J_z - I_y - J_y}{I_x + J_x},\ j_2 = \frac{J_z - J_x - J_y}{I_x + J_x},\ j_3 = \frac{J_y + J_x - J_z}{J_y}, \tag{8}$$

$$j_4 = \frac{2J_z - 2J_x}{I_x + J_x},\ w^2 = \frac{\omega_2^2}{\omega_1^2},$$

where $\omega_1 = \sqrt{\frac{k_{11}}{I_x + J_x}}$, $\omega_2 = \sqrt{\frac{k_{21}}{J_y}}$.

The dimensionless form of the governing equations takes the following form

$$\phi + \left(1 + j_1 \omega_z^2\right)\phi - \alpha_1 \phi^3 + c_1 \phi + j_2 \omega_z \vartheta + j_4 \vartheta \vartheta \phi = f_0 \sin\left(p\tau\right), \tag{9}$$

$$\vartheta + \left(w^2 + \left(1 - j_3\right)\omega_z^2\right)\vartheta - \alpha_2 \vartheta^3 + c_2 \vartheta + \left(1 - j_3\right)\omega_z \vartheta^2 \varphi + \left(j_3 - 1\right)\vartheta \varphi^2 + j_3 \omega_z \varphi = 0, \tag{10}$$

where functions $\varphi(\tau)$, $\vartheta(\tau)$ correspond to the dimensional general coordinates $\Phi(t)$ and $\Theta(t)$. Equations (9) and (10) are supplemented with the proper initial conditions

$$\varphi(0) = \varphi_0,\ \dot{\varphi}(0) = \omega_0,\ \vartheta(0) = \vartheta_0,\ \dot{\vartheta}(0) = \varpi_0. \tag{11}$$

From the viewpoint of the gyroscope applications, the main resonance is the most important state of its work. Ideally, it is desired to utilize resonance in both the drive and the sense modes in order to attain the maximum possible response gain and sensitivity. This is typically achieved by properly designing and if needed tuning the resonant frequencies of the drive and the sense in order to their equalizing. This is why we have assumed that $\omega_2 = \omega_1$ (i.e. w=1). Angular velocity of the substrate ω_z is usually much lower than angular frequencies of the movable gyroscope elements. Therefore, in order to deal with this case of the resonance we take

$$p = 1 + \sigma, \tag{12}$$

where σ plays a role of the detuning parameter.

4. Approximate analytical solution

The method of multiple scales (MSM) has been used to solve of the problem (9) – (11) taking into account the main resonance condition. Since a few of the parameters are assumed to be small, after introduction of the so-called small/perturbation parameter ε the following relations are employed:

$$c_1 = \tilde{c}_1 \varepsilon^2,\ c_2 = \tilde{c}_2 \varepsilon^2,\ w_z = \tilde{w}_z \varepsilon,\ f_0 = \tilde{f}_0 \varepsilon^3,\ \sigma = \tilde{\sigma} \varepsilon^2. \tag{13}$$

According to MSM, three time scales are introduced that are defined in the following manner: $\tau_0 = \tau$ is the "fast" time, whereas $\tau_1 = \varepsilon\tau$ and $\tau_2 = \varepsilon^2\tau$ serve as the "slow" times [3]. The derivatives with respect to time τ are calculated in terms of the new time scales as follows

$$\begin{aligned}&\frac{d}{d\tau} = \frac{\partial}{\partial\tau_0} + \varepsilon\frac{\partial}{\partial\tau_1} + \varepsilon^2\frac{\partial}{\partial\tau_2},\\ &\frac{d^2}{d\tau^2} = \frac{\partial^2}{\partial\tau_0^2} + 2\varepsilon\frac{\partial^2}{\partial\tau_0\partial\tau_1} + \varepsilon^2\left(\frac{\partial^2}{\partial\tau_1^2} + 2\frac{\partial^2}{\partial\tau_0\partial\tau_2}\right) + o\left(\varepsilon^3\right).\end{aligned} \tag{14}$$

The solution of the initial-value problem (9) – (11) is searched in the form of the power series regarding the small parameter ε:

$$\varphi(\tau;\varepsilon) = \sum_{k=1}^{k=3}\varepsilon^k\phi_k(\tau_0,\tau_1,\tau_2) + O(\varepsilon^4), \qquad \vartheta(\tau;\varepsilon) = \sum_{k=1}^{k=3}\varepsilon^k\theta_k(\tau_0,\tau_1,\tau_2) + O(\varepsilon^4). \tag{15}$$

Then, relations (13) – (14) are introduced into equations of motion (9) - (10). In this way, the small parameter appears in the mathematical model. After rearranging the equations with respect to the powers of the small parameter, we get a system of equations which are to be satisfied in order to guarantee satisfaction to the original equations. They are as follows:

- the equations of the first order approximation

$$\frac{\partial^2\phi_1}{\partial\tau_0^2} + \phi_1 = 0, \tag{16}$$

$$\frac{\partial^2\theta_1}{\partial\tau_0^2} + \theta_1 = 0; \tag{17}$$

- the equations of the second order approximation

$$\frac{\partial^2\varphi_2}{\partial\tau_0^2} + \varphi_2 = -2\frac{\partial^2\varphi_1}{\partial\tau_0\partial\tau_1}, \tag{18}$$

$$\frac{\partial^2\theta_2}{\partial\tau_0^2} + \theta_2 = -2\frac{\partial^2\theta_1}{\partial\tau_0\partial\tau_1}; \tag{19}$$

- the equations of the third order approximation

$$\begin{aligned}&\frac{\partial^2\varphi_3}{\partial\tau_0^2} + \varphi_3 = -2\frac{\partial^2\varphi_1}{\partial\tau_0\partial\tau_2} - 2\frac{\partial^2\varphi_2}{\partial\tau_0\partial\tau_1} - \frac{\partial^2\varphi_1}{\partial\tau_1^2} + \alpha_1\varphi_1^3 - c_1\frac{\partial\varphi_1}{\partial\tau_0} -\\ &j_4\theta_1\frac{\partial\theta_1}{\partial\tau_0}\frac{\partial\varphi_1}{\partial\tau_0} - j_2\omega_z\frac{\partial\theta_1}{\partial\tau_0} + f_0\sin(\tau_0 + \tau_2\sigma),\end{aligned} \tag{20}$$

$$\frac{\partial^2\theta_3}{\partial\tau_0^2}+\theta_3=-2\frac{\partial^2\theta_1}{\partial\tau_0\partial\tau_2}-2\frac{\partial^2\theta_2}{\partial\tau_0\partial\tau_1}-\frac{\partial^2\theta_1}{\partial\tau_1^2}+\alpha_2\theta_1^3-c_2\frac{\partial\theta_1}{\partial\tau_0}- \tag{21}$$
$$j_3\theta_1\left(\frac{\partial\varphi_1}{\partial\tau_0}\right)^2-j_3\omega_z\frac{\partial\varphi_1}{\partial\tau_0}+\theta_1\frac{\partial\varphi_1}{\partial\tau_0}.$$

System (16) – (21) is solved recursively, i.e. solution of equations (16) – (17) is substituted into equations (18) – (19), and then their solution into equations (20) – (21). The solution contains unknown complex functions $B_1(\tau_1,\tau_2)$ and $B_2(\tau_1,\tau_2)$. The values of generalized coordinates are to be bounded, therefore all secular terms should be eliminated what leads to conclusion that $B_1(\tau_2)$ and $B_2(\tau_2)$ do not depend on the time scale τ_1 and satisfy the solvability condition:

$$-j_4\overline{B}_1B_2^2-iB_1\tilde{c}_1-\frac{1}{2}ie^{i\tau_2\tilde{\sigma}}f_0+3B_1^2\overline{B}_1\tilde{\alpha}_1-i\,j_2B_2\tilde{\omega}_z=2i\frac{dB_1}{d\tau_2}, \tag{22}$$

$$2(1-j_3)B_1\overline{B}_1B_2+(j_3-1)B_1^2\overline{B}_2-iB_2\tilde{c}_2+3B_2^2\overline{B}_2\tilde{\alpha}_2-i\,j_3B_1\omega_z=2i\frac{dB_2}{d\tau_2}. \tag{23}$$

The functions $B_1(\tau_2)$ and $B_2(\tau_2)$ can be determined from the solvability conditions (22) – (23), but it is more preferably to introduce their real representations as follows

$$B_1(\tau_2)\to\frac{\tilde{a}_1(\tau_2)}{2}e^{i\psi_1(\tau_2)},\qquad B_2(\tau_2)\to\frac{\tilde{a}_2(\tau_2)}{2}e^{i\psi_2(\tau_2)}, \tag{24}$$

where $a_1=\varepsilon\tilde{a}_1$, $a_2=\varepsilon\tilde{a}_2$ and ψ_1, ψ_2 are real-valued functions and denote amplitudes and phases of the general coordinates φ and ϑ.

After substituting (24) into (22) – (23) and separating real and imaginary parts, we obtain the modulation equations which can be transformed to more suitable autonomous form by introducing modified phases as follows

$$\psi_1(\tau_2)=\tau_2\tilde{\sigma}-\Psi_1(\tau_2),\quad \psi_2(\tau_2)=\tau_2\tilde{\sigma}-\Psi_2(\tau_2)\ \text{ and }\ \sigma=\varepsilon^2\tilde{\sigma}. \tag{25}$$

Substituting expressions (24) and (25) into the solvability conditions (22) – (23) and returning to the initial denotations according to (13), the modulation equations in autonomous form are obtained

$$a_1\frac{\partial\Psi_1}{\partial\tau}=a_1\sigma-\frac{1}{8}j_4a_1a_2^2\cos(2(\Psi_1-\Psi_2))+\frac{1}{2}j_2\omega_za_2\sin(\Psi_1-\Psi_2)+\frac{1}{2}f_0\sin(\Psi_1), \tag{26}$$

$$\frac{\partial a_1}{\partial\tau}=-\frac{1}{2}c_1a_1-\frac{1}{8}j_4a_1a_2^2\sin(2(\Psi_1-\Psi_2))-\frac{1}{2}j_2\omega_za_2\cos(\Psi_1-\Psi_2)-\frac{1}{2}f_0\cos(\Psi_1), \tag{27}$$

$$a_2\frac{\partial\Psi_2}{\partial\tau}=a_2\sigma+\frac{1-j_3}{4}a_1^2a_2+\frac{3}{8}\alpha_2a_2^3+\frac{1}{8}(j_3-1)a_1^2a_2\cos(2(\Psi_1-\Psi_2))-\frac{1}{2}j_3\omega_za_1\sin(\Psi_1-\Psi_2), \quad (28)$$

$$\frac{\partial a_2}{\partial\tau}=-\frac{1}{2}c_2a_2-\frac{1}{2}j_3\omega_za_1\cos(\Psi_1-\Psi_2)+\frac{1-j_3}{8}a_1^2a_2\sin(2(\Psi_1-\Psi_2)). \quad (29)$$

There is no possibility to solve analytically the modulation equations (26) – (29). The final form of the analytical solution of the original problem (9) – (11) is obtained after substituting solutions of equations (16) – (21) into power series (15):

$$\varphi=a_1\cos(\tau+\psi_1)-\frac{1}{32}\alpha_1a_1^3\cos(3(\tau+\psi_1))-\frac{1}{32}j_4a_1a_2^2\cos(3\tau+\psi_1+2\psi_2), \quad (30)$$

$$\vartheta=a_2\cos(\tau+\psi_2)-\frac{1}{32}\alpha_2a_2^3\cos(3(\tau+\psi_2))+\frac{1-j_3}{32}a_1^2a_2\cos(3\tau+2\psi_1+\psi_2), \quad (31)$$

where a_1, a_2, ψ_1 and ψ_2 satisfy modulation equations (26) – (29).

Taking into account some special case of parameters discussed in [4], i.e. $j_4=0$, $j_2=-1$ and $j_3=1$, the amplitude-frequency response functions are obtained analytically. They follow

$$9a_2^6\alpha_2^2+48a_2^4\alpha_2\sigma+a_2^2(16c_2^2+64\sigma^2)=16a_1^2w_z^2, \quad (32)$$

$$9a_1^8\alpha_1^2+48a_1^6\alpha_1\sigma+2a_1^4(8c_1^2-9a_2^4\alpha_1\alpha_2-24a_2^2\alpha_1\sigma+32\sigma^2)-16a_1^2a_2^2(\sigma(3a_2^2\alpha_2+8\sigma)-2c_1c_2)+a_2^4(16c_2^2+(3a_2^2\alpha_2+8\sigma)^2)=16a_1^2f_0^2. \quad (33)$$

The derived formulas (32) – (33) offer a well-judged analysis of the influence of parameters on the steady state vibration of the gyroscope sensing plate.

5. Results

Here are presented some exemplary graphs concerning motion of the gyroscope near resonance. Calculations are performed for the following fixed dimensionless parameters: $\omega_z=6.64\times10^{-5}$, $f_0=4.37\times10^{-7}$, $c_1=c_2=3.98\times10^{-5}$, $\alpha_1=\alpha_2=1$, $j_1=-1.6\times10^{-16}$, $j_2=-1$, $j_3=1$, $j_4=0$. The latter correspond to values of real-world structure [4]. Time histories of the generalized coordinates φ and ϑ, according to (30) – (31), are presented in Fig. 3.

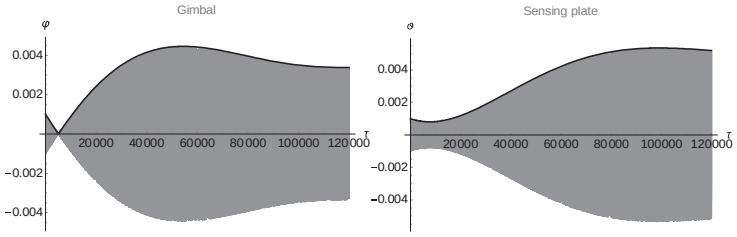

Figure 3. Time histories of the vibration.

The thick black line in Fig. 3 describe amplitude modulation yielded by equations (26) – (29). It should be emphasized that the approximate analytical solution satisfies the governing equations (9) – (10) with a high accuracy (the absolute errors Δ_1 and Δ_2 are reported in Fig. 4).

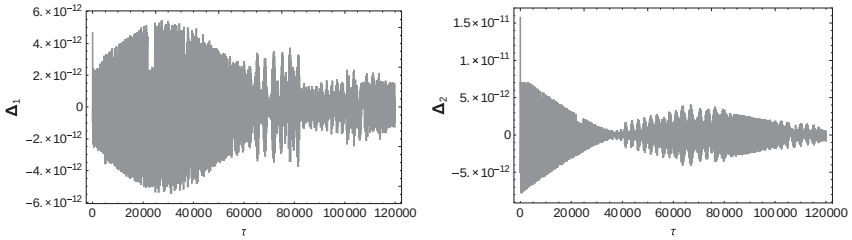

Figure 4. Absolute errors exhibited by the governing equations for the approximate analytical solution.

The employed analytical methodology and computational approach is suited to engineers dealing with MEMS. Namely, we have used the optimized numerical algorithm implemented in Wolfram Mathematica^{TM}. However, in the latter case the error of satisfaction of the equation of motion is five orders of magnitude larger in comparison to our described analytical solutions.

The amplitude curves for steady state motion obtained with the help of eq. (32) – (33) are presented in Fig. 5 for the same data as before.

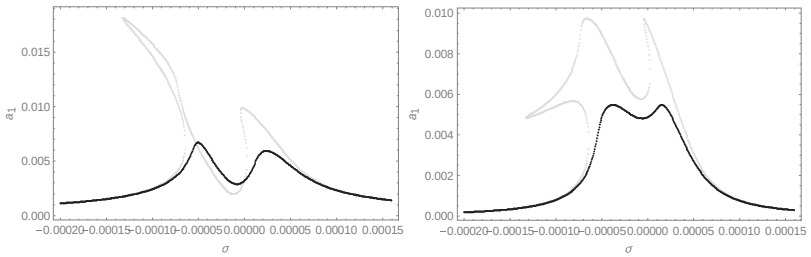

Figure 5. Amplitude of steady state vibration vs. detuning parameter: grey line – small damping $c_1 = c_2 = 2.2\times10^{-5}$; black line – large damping $c_1 = c_2 = 4.0\times10^{-5}$

For small value of the damping coefficients several regimes of steady-state amplitudes are possible. On the other hand, for properly large damping coefficients, the amplitudes versus time create the unique functions.

6. Conclusions

The mathematical model describing dynamics of some class of micromechanical gyroscope has been derived and presented in dimensionless form. The approximate analytical solution of the governing equations has been obtained using multiple scale method in time domain in the case of main resonance. The analytical solution presented in compact form gives opportunity to study behavior of the system for wide range of parameters. The asymptotic solution is very accurate.

The analytical form of the amplitude-frequency dependence allows to qualitative and quantitative analysis of the steady-state motion of the system. The results show, among others, that value of damping coefficients may violate uniqueness of the solution and influence the duration of the transient states.

Acknowledgments

This paper was financially supported by the grant of the Ministry of Science and Higher Education in Poland realized in Institute of Applied Mechanics of Poznan University of Technology (DS-PB: 02/21/DSPB/3493).

References

[1] Williams C.B., Shearwood C., Mellor P.H., Mattingley A.D., Gibbs M.R., Yates R.B., Initial fabrication of a micro-induction gyroscope, Microelectron. Eng. 30 (1996) 531–534.

[2] Jin L., Zhang H., Zhong Z., Design of a lc-tuned magnetically suspended rotating gyroscope, J. Appl. Phys. 109 (2011) 07E525–07E525–3.

[3] Awrejcewicz J., Krysko V. A.: *Introduction to Asymptotic Methods*, Boca Raton, Chapman and Hall, 2006.

[4] Merkuriev I.W, Podalkov W.W.: Study of nonlinear dynamics of a micromechanical gyroscope. Pproceedings of the IV International School –NDM “Nonlinear Dynamics of Machines”, 82-91, IMASH RAS, Moscow 2017 (in Russian)

Roman Starosta, Ph. D: Poznań University of Technology, Institute of Applied Mechanics, ul. Piotrowo 3, 60-965 Poznań, Poland (*roman.starosta@put.poznan.pl*). The author gave a presentation of this paper during one of the conference sessions.

Jan Awrejcewicz, Professor: Technical Universityof of Łódź, Department of Automatics and Biomechanics, ul. Stefanowskiego 90-924, Łódź, Poland (*awrejcew@p.lodz.pl*).

Grażyna Sypniewska-Kamińska, Ph. D: Poznań University of Technology, Institute of Applied Mechanics, ul. Piotrowo 3,60-965 Poznań, Poland, (*grazyna.sypniewska-kaminska@put.poznan.pl*).